

2015, 2017, 2017

which should be cited to refer to this work.

## Experimental Section

### Inorganic Synthesis

All chemicals were purchased from Sigma-Aldrich (Switzerland) and used without additional purification unless otherwise specified. mPEG-SH was purchased from Creative PEGWorks.

### Synthesis of GNRs

The synthetic route was similar to that previously published with an increased scale.<sup>1</sup> A seed-mediated route was used whereby the concentration of silver ions could be used to tune the aspect ratio of the GNRs.

Briefly, a CTAB solution (0.1 M, 4.7 mL) was mixed with  $\text{HAuCl}_4 \cdot 3\text{H}_2\text{O}$  (50 mM, 0.025 mL) at 28°C. To this stirred solution, freshly prepared  $\text{NaBH}_4$  (10 mM, 0.6 mL) was added. While aging the seeds for 1h, a growth solution was prepared. This consisted of consecutive additions, with inversion mixing between additions, of CTAB (0.1 M, 400 mL),  $\text{HAuCl}_4 \cdot 3\text{H}_2\text{O}$  (50 mM, 4.44 mL),  $\text{AgNO}_3$  (10 mM, 5.2 mL), and  $\text{HCl}$  (1 M, 7.68 mL). L-ascorbic acid (0.1 M, 3.2 mL) was then added followed by vigorous mixing until the solution turned colourless. The seed particles (1.92 mL) were initially dosed into the foam created by the mixing of the growth solution, before vigorous inversion mixing for 1 min. The suspension was left overnight at 28 °C to let GNRs form.

### Characterization of GNRs

TEM images were taken using a Phillips CM20 Biotwin operating at 80 kV (Figure S1a). The suspension was washed twice via centrifugation (1 ml centrifuged twice 8,000 x g for 5 minutes) and redispersed in water. This suspension was drop cast onto a TEM grid and dried in air. A minimum of 200 particles were analyzed to obtain the size distribution, summarized in Table S1.

The UV-Vis-NIR spectrum was measured on a Jasco V-670 spectrophotometer, with the suspension diluted 1:10 in water (Figure S1b). Zeta-potential measurements were made on a Brookhaven ZetaPALS (Table S1). To assess the concentration, an aliquot of the GNR suspension was washed twice, as described above, before dissolution in aqua regia. The treated samples were then measured by ICP-OES using a PerkinElmer Optima 7000 DV (Table S1).

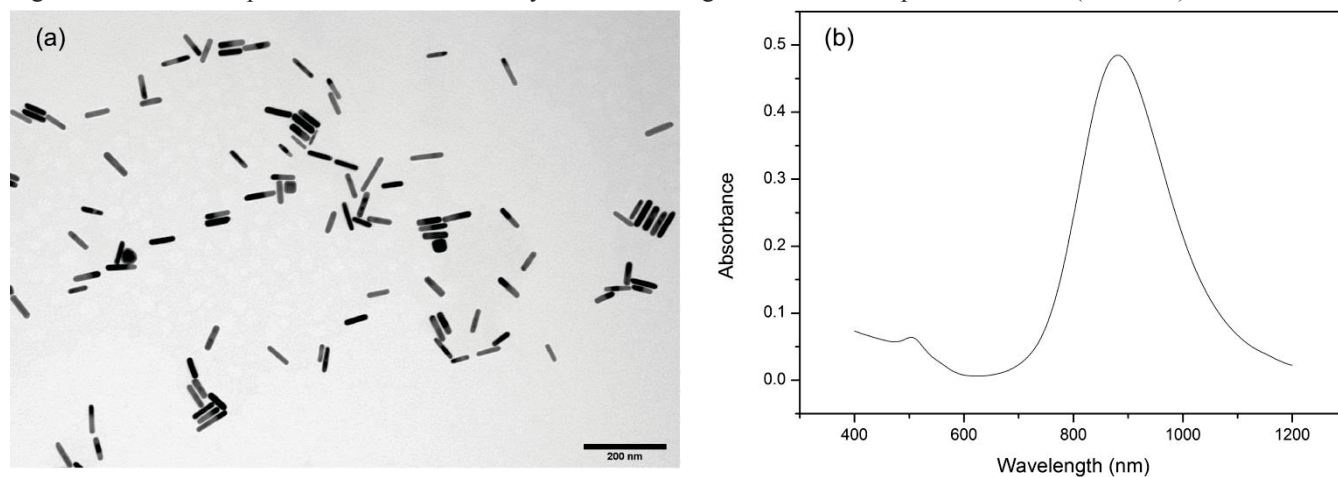


**Figure S1.** (a) TEM of GNRs after washing twice by centrifugation and redispersion in water. (b) UV-Vis-NIR spectra of 10x diluted GNR suspension.

**Table S1.** GNR characteristics.

Property	Value
Dimensions (TEM)	$57 \pm 10 \times 12 \pm 2$ nm
Aspect Ratio (TEM)	$4.7 \pm 1$

Shape yield of nanorods to spheres	96 %
Mean surface area per GNR	2216 ± 625 nm <sup>2</sup>
Mean volume per GNR	6525 ± 2771 nm <sup>3</sup>
Extinction coefficient (at 400 nm)	0.0145 μg <sup>-1</sup> .mL.cm <sup>-1</sup>
Zeta-potential	+35.5 ± 2.5 mV

## Organic Synthesis

All chemicals were purchased from Sigma-Aldrich (Switzerland) and used without additional purification unless otherwise specified. Vinyl acetate was freshly distilled to remove polymerization inhibitors. N-methoxycarbonylmaleimide and carbon disulfide were purchased from Acros and ethanol was from VWR. Deuterated solvents were obtained from Cambridge Isotope Laboratory. Thin layer chromatography (TLC) plates were purchased from Merck.

All reactions were carried out under inert atmosphere using Argon flux and all reactants were added via syringe. Solvent was removed by rotary evaporation at 40 °C and compounds were dried under high vacuum on a Schlenk-line.

### Instrumentation

Visualization after TLC was performed with a 254 nm or 365 nm UV lamp. Flash column chromatography was performed on an Isolera One from Biotage. <sup>1</sup>H NMR spectra were recorded on a Bruker Avance DPX 300 MHz spectrometer. Chemical shifts were expressed in parts per million (ppm; δ) and referenced internally to the residual solvent signal. Coupling constants (J) are reported in Hz. Multiplets are abbreviated as follows: s (singlet), d (doublet), dd (doublet of doublet), t (triplet), m (multiplet).

GPC in THF was carried out on an Agilent Technologies 1200 Series system at 40 °C with a flow rate of 1.0 mL/min using multiangle laser light scattering (λ = 658 nm, 25 °C) and refractive index detectors. A Polymer Laboratories 5 μm mixed-C guard column and two GPC columns of Wyatt Technology Corp. (Optilab REX interferometric refractometer, miniDawn TREOS laser photometer) were used. The incremental refractive index (dn/dc) was estimated by a single-injection method that assumed 100% mass recovery from the columns.

### Ethyl 2-(ethoxythiocarbonylthio) propanoate (**1**)

To a stirred solution of potassium hydroxide (13 g, 232.0 mmol, 1.0 eq.) in ethanol (100 g), carbon disulfide (18 g, 236.8 mmol, 1.0 eq.) was added dropwise. After stirring for 2 h, the solution was cooled to 5 °C, filtered and the crude product recrystallized twice from warm ethanol, giving a yellow powder (**1**). Yield: 24.2 g, 150.9 mmol, 65.0%.

### Ethyl 2-((ethoxycarbonothioyl)thio)propanoate (**2**)

Ethyl-2-bromo propionate (10.6 g, 58.6 mmol, 1.0 eq.) in dry acetonitrile (2 mL) was cooled to 0 °C and potassium ethyl xanthogenate (**1**) (10 g, 62.4 mmol, 1.1 eq.) was added portionwise. The suspension was stirred at RT for 2 h before the solvent was removed under reduced pressure. After redissolving in dichloromethane, the organic phase was washed with water and brine, dried over magnesium sulfate and concentrated. The crude product was purified via column chromatography with hexane: diethylether (19:1 to 9:1) as eluent giving a colorless liquid (**2**). Yield: 8.1 g, 36.4 mmol, 62.1%.

<sup>1</sup>H NMR (300 MHz, CHLOROFORM-d) δ [ppm]: 4.63 (q, J=7.18 Hz, 2 H), 4.37 (q, J=7.37 Hz, 1 H), 4.20 (q, J=7.18 Hz, 2 H), 1.56 (d, J=7.55 Hz, 3 H), 1.41 (t, J=7.18 Hz, 3 H), 1.28 (t, J=7.08 Hz, 3 H)

### RAFT polymerization of vinyl acetate (**3**)

A mixture of freshly distilled vinyl acetate (40 g, 465.1 mmol, 116.3 eq.), AIBN (65.9 mg, 0.4 mmol, 0.1 eq.) and ethyl 2-(ethoxythiocarbonylthio) propanoate (**2**, 888.0 mg, 4.0 mmol, 1.0 eq.) was degassed and fully immersed in an

oil bath pre-heated to 70 °C. The polymerization was quenched after 23 h, before dissolving the polymer in dichloromethane and precipitating in a 10-fold excess of ice-cold hexane (**3**).

<sup>1</sup>H-NMR (300 MHz, CHLOROFORM-d) δ [ppm]: 4.90 (s, CH backbone), 4.70-4.55 (m, 2H, S=COCH<sub>2</sub>CH<sub>3</sub> RAFT agent moiety), 4.20-4.10 (m, 2H, O=COCH<sub>2</sub>CH<sub>3</sub> RAFT agent moiety), 2.15-1.95 (m, CH<sub>3</sub> backbone), 1.95-1.60 (m, CH<sub>2</sub> backbone), 1.45-1.35 (m, 3H, O=COCH<sub>2</sub>CH<sub>3</sub> RAFT agent moiety), 1.30-1.20 (m, 3H, S=COCH<sub>2</sub>CH<sub>3</sub> RAFT agent moiety), 1.20-1.10 (m, 3H, O=CCHCH<sub>3</sub> RAFT agent moiety) 0.90-0.80 (m, H, O=CCHCH<sub>3</sub> RAFT agent moiety).

#### Thiol end-functional poly(vinyl acetate) (**4**)

To generate the thiol moiety, the procedure described by Hien The Ho *et al.* was modified.<sup>2</sup> A mixture of poly(vinyl acetate) (**3**, 40 g, 2.7 mmol, 1.0 eq.), in dichloromethane (200 mL) was degassed. Degassed n-hexylamine (60 mL, 456.6 mmol, 169.1 eq.) was added dropwise and stirred during 2.5 h at RT under inert atmosphere. The polymer, dissolved in dichloromethane, was precipitated in a 10-fold excess of ice-cold hexane (**4**).

<sup>1</sup>H-NMR (300 MHz, CHLOROFORM-d) δ [ppm]: 4.90 (s, CH backbone), 4.20-4.10 (m, 2H, O=COCH<sub>2</sub>CH<sub>3</sub> RAFT agent moiety), 2.15-1.95 (m, CH<sub>3</sub> backbone), 1.95-1.60 (m, CH<sub>2</sub> backbone), 1.45-1.35 (m, 3H, O=COCH<sub>2</sub>CH<sub>3</sub> RAFT agent moiety), 1.30-1.20 (m, 3H, S=COCH<sub>2</sub>CH<sub>3</sub> RAFT agent moiety), 1.20-1.10 (m, 3H, O=CCHCH<sub>3</sub> RAFT agent moiety) 0.90-0.80 (m, H, O=CCHCH<sub>3</sub> RAFT agent moiety).

#### NMR Spectra

<sup>1</sup>H NMR spectra were recorded on a Bruker Avance DPX 300 MHz spectrometer. Chemical shifts were expressed in parts per million (ppm; δ) and referenced internally to the residual solvent signal. Coupling constants (J) are reported in Hz. Multiplets are abbreviated as follows: s (singlet), d (doublet), dd (doublet of doublet), t (triplet), m (multiplet).

GPC in THF was carried out on an Agilent Technologies 1200 Series system at 40 °C with a flow rate of 1.0 mL.min<sup>-1</sup> using multiangle laser light scattering (λ = 658 nm, 25 °C) and refractive index detectors. A Polymer Laboratories 5 μm mixed-C guard column and two GPC columns of Wyatt Technology Corp. (Optilab REX interferometric refractometer, miniDawn TREOS laser photometer) were used. The incremental refractive index (dn/dc) was estimated by a single-injection method that assumed 100% mass recovery from the columns.

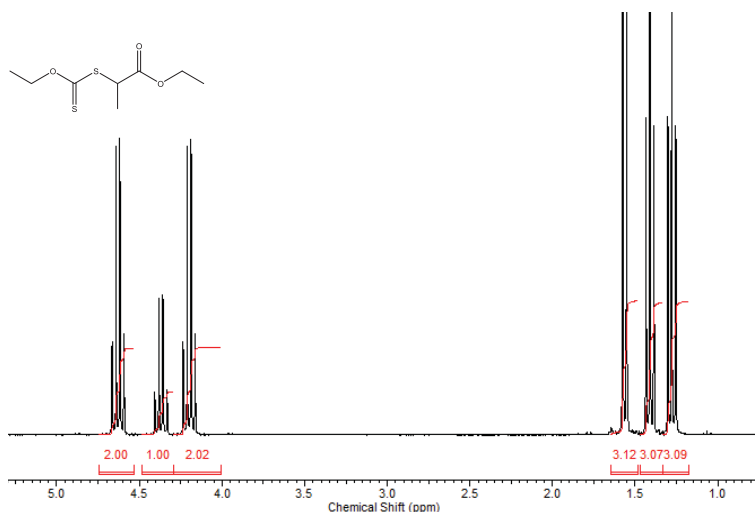


**Figure S2.** <sup>1</sup>H-NMR spectrum of ethyl 2-(ethoxythiocarbonylthio) propanoate (**2**).

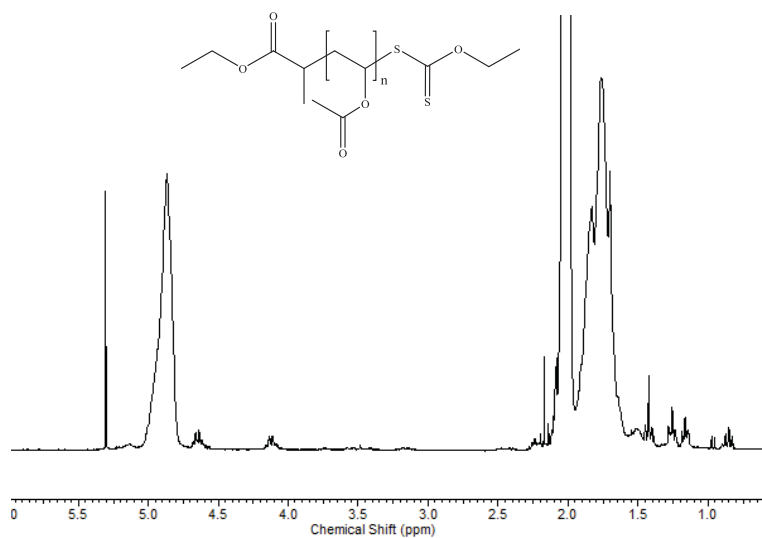


**Figure S3.** <sup>1</sup>H-NMR spectrum of poly(vinyl acetate) (3).

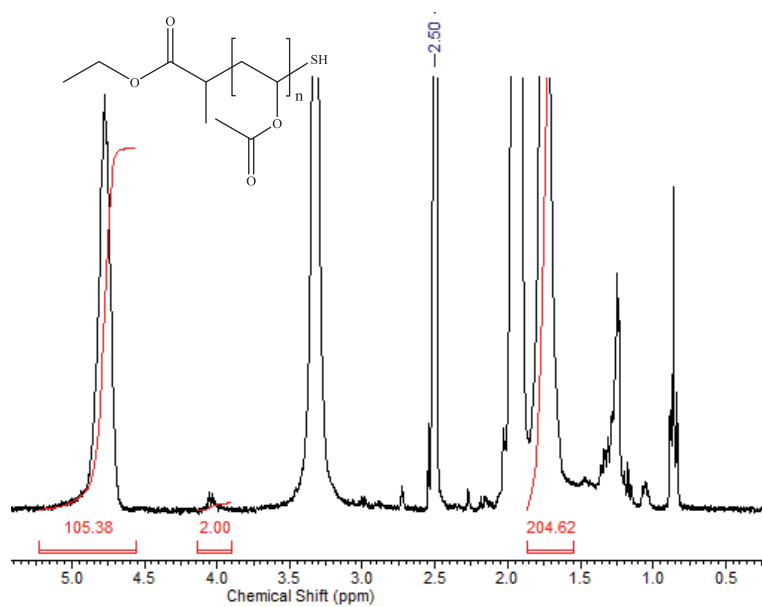


**Figure S4.** <sup>1</sup>H-NMR spectrum of thiolated poly(vinyl acetate) (4).

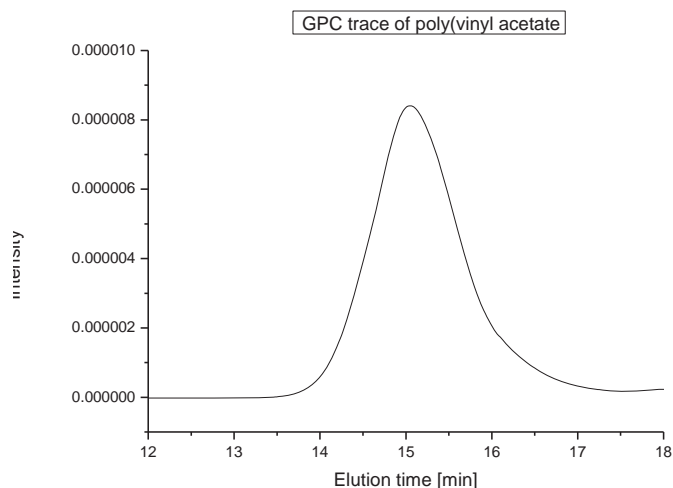


**Figure S5.** GPC trace of poly(vinyl acetate) in THF (**3**).

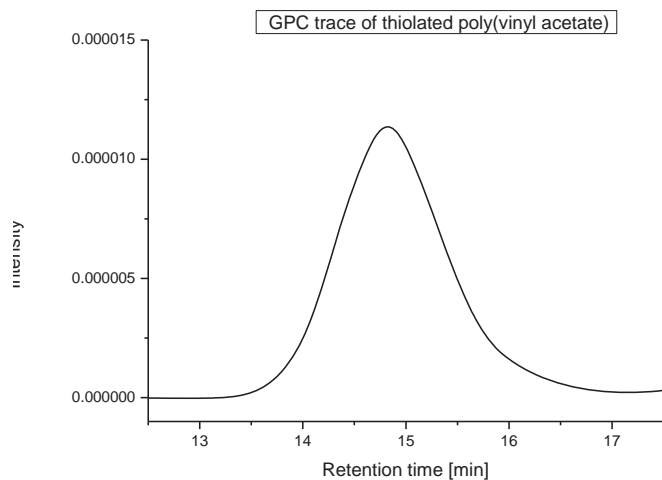


**Figure S5.** GPC trace of thiolated poly(vinyl acetate) in chloroform (**4**).

**Table S2.** Calculated molecular weights from GPC traces before and after aminolysis of poly(vinyl acetate).

	$M_n$ (Da)	$M_w$ (Da)	PDI
PVAc ( <b>3</b> )	15,100	20,000	1.3
Thiolated PVAc ( <b>4</b> )	25,900	36,000	1.4

### Functionalization of GNRs

#### PVA functionalization

The GNRs, 20 mL of the suspension as synthesized, were centrifuged at 8,000  $\times$ g for 20 minutes. The supernatant was removed and the pellet redispersed in 1 mL of the remaining liquid. This was then added dropwise over a period of 15 min under vigorous stirring to a solution of end-thiolated PVAc in DMF (0.116 g PVAc in 20 mL DMF). Stirring was then stopped and the suspension left overnight at RT before upconcentrating by centrifugation to 0.21 mL.

The concentrated GNRs were added dropwise to a stirred solution of end-thiolated PVAc in methanol/ethanol (58 mg PVAc in 50% v/v MeOH/EtOH) over a period of 15 min. This was left to react for 3 h before transferring the suspension to basic methanol (0.25 M NaOH in 10 mL MeOH) via centrifugation. The suspension was heated to 65 °C with magnetic agitation, until a precipitate was observed – between 1 and 3 h. This precipitate was washed with methanol until the pH returned to neutral. Upon addition of a small quantity of water, the GNRs instantly dispersed into suspension. The stable suspension was stored at 4 °C until use.

#### PEG functionalization

A similar route to that previously published was followed.<sup>1</sup> Briefly, 20 mL of the GNRs suspension, as synthesized, was centrifuged (8,000 ×g for 20 min) and redispersed in 20 mL of water giving a CTAB concentration of 1 mM. A solution of mPEG-SH (3.952 mL of 1 mg.mL<sup>-1</sup> mPEG-SH, 5 kDa, in water) was added and left to react overnight at RT.

The suspension was centrifuged and the pellet redispersed in mPEG-SH in ethanol (20 mL of 0.2 mg.mL<sup>-1</sup> mPEG-SH in 90% v/v EtOH/H<sub>2</sub>O) before leaving the suspension to react overnight at RT. The PEGylated GNRs were washed three times by centrifugation into water, and stored at 4 °C.

#### Characterization of PVA-GNRs

##### UV-Visible spectroscopy

UV-Visible spectroscopy was carried out on a Jasco V-670 spectrophotometer; Depolarized Dynamic Light Scattering (DDLS) on a 3D LS spectrometer (LS Instruments); Zeta-potential measurements on a 90Plus PALS (Brookhaven Instruments Cooperation).

The UV-Vis spectra of the CTAB and PVA stabilized GNRs are shown in Figure S6.

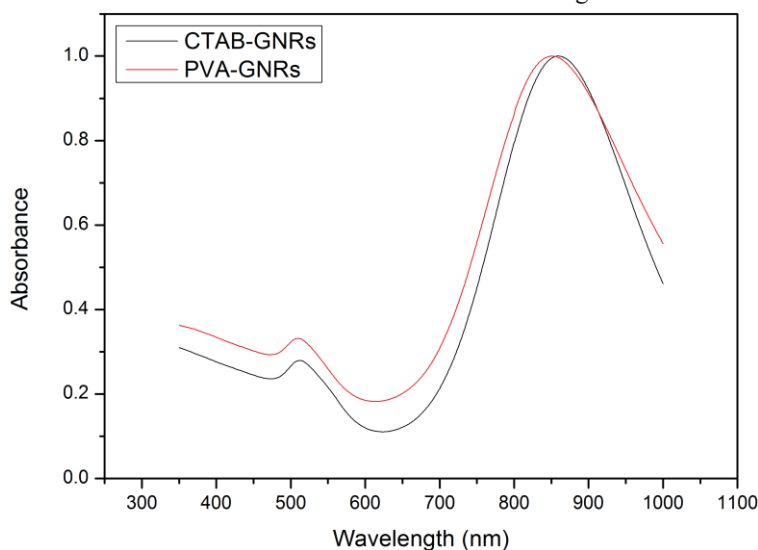


**Figure S6.** UV-Visible spectra of CTAB-GNRs in water and PVA-GNRs in water.

The concentration of PVAc and CTAB in the functionalization step in DMF was investigated by UV-Visible spectroscopy. When no PVAc was added to the DMF, aggregation of the GNRs occurred although the presence of extra CTAB resulted in far lower colloidal stability suggesting the DMF stabilizes a monolayer of CTAB (Figure S7a). Upon varying the concentration of PVAc in DMF during the initial functionalization step (10, 100, or 1000 PVAc per nm<sup>-2</sup> of GNR surface area), varying degrees of stability were found as shown in Figure S7b.

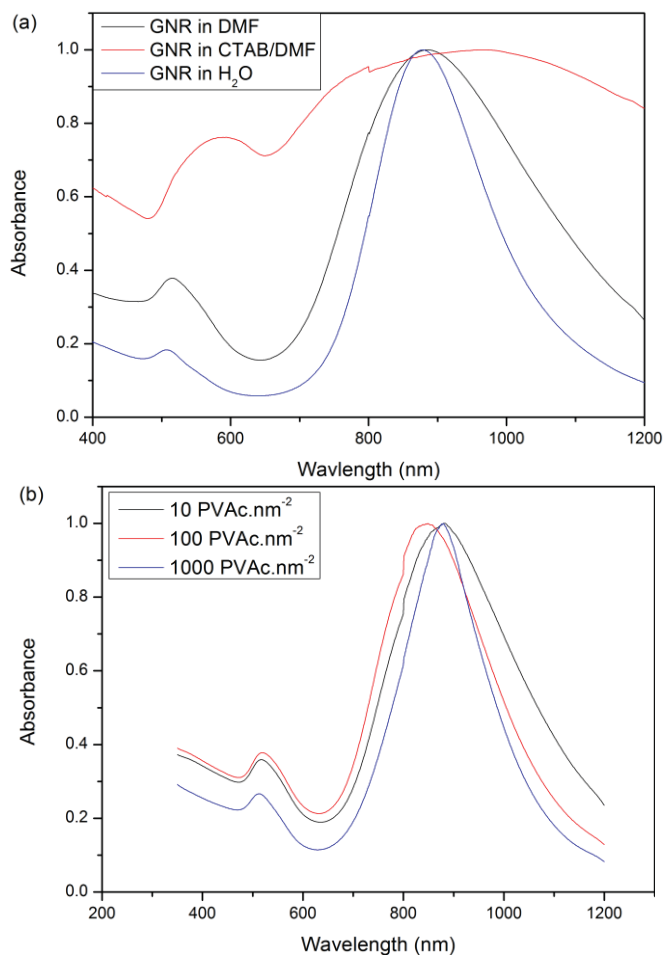


**Figure S7.** (a) UV-Visible spectra of GNRs added to either pure DMF, a solution of CTAB in DMF, or water. (b) UV-Visible spectra of GNRs added to a solution of end-thiolated PVAc in DMF where the concentration of PVAc was varied from 10 to 1000 PVAc per nm<sup>2</sup> of GNR surface area.

### Hydrophobicity

The hydrophobicity of the suspension of PVAc functionalized GNRs in methanol/ethanol was crudely assessed by added water up to 10% v/v. Instantaneous aggregation was observed, shown in Figure S8.



**Figure S8.** GNRs functionalized with end-thiolated PVAc in DMF (left) with a residual water concentration of 1% v/v. Upon addition of water to 12% v/v, the GNRs aggregated (right).

### Zeta-potential

The zeta-potential of the suspension at different stages of the functionalization procedure are given in Table S3.

**Table S3.** The zeta-potential of the GNR suspension at different stages of the functionalization with each suspension aged for 24 h in the reaction mixture before measuring.

Sample	Zeta-potential (mV)
GNR-CTAB in water	+ 35.5
GNR-PVAc in DMF	+ 1.2
GNR-PVAc in EtOH	- 1.4
GNR-PVA in water	- 19.1

### DDLS

Two Glan-Thompson polarizers with extinction coefficients better than  $10^{-6}$  and  $10^{-8}$  were placed in the path of the incoming laser and before the detector, respectively. When these polarizers are crossed, the collected autocorrelation function originates from optically anisotropic objects in the sample allowing the investigation of both rotational and translational dynamics. We collected the autocorrelation functions at a number of scattering vectors,  $q$ , from  $1.12 \times 10^{-2}$  to  $2.29 \times 10^{-2} \text{ nm}^{-1}$ , where  $q$  is defined by

$$q = \frac{4\pi n}{\lambda} \sin\left(\frac{\theta}{2}\right) \quad (1)$$

where  $n$  is the refractive index,  $\lambda$  is the incident laser wavelength, and  $\theta$  is the scattering angle.

It is known that the decay rate of the autocorrelation function in DDLS is linearly proportional to  $q$ , via the relation

$$\Gamma = D_T q + 6D_R \quad (2)$$

where  $\Gamma$  is the decay rate, obtained via an exponential fit to the autocorrelation function,  $D_T$  is the translational diffusion coefficient and  $D_R$  is the rotational diffusion coefficient.<sup>3</sup>

It was found that the polydispersity (17% in length and 17% in width) could be accurately described for the entire autocorrelation function by a 3<sup>rd</sup> order cumulant fit (Figure S9). Therefore, the decay rate was calculated using this fit and was plotted as a function of  $q$  (Figure 2a). The gradient of the slope gave a translational diffusion coefficient of  $D_T = 6.81 \times 10^{-12} \text{ m}^2 \cdot \text{s}^{-1}$ , while the intercept gave a rotational diffusion coefficient of  $D_R = 4327 \text{ s}^{-1}$ .

In order to transform these coefficients into corresponding hydrodynamic parameters, a theoretical model is needed. We chose to apply the spherocylindrical model as it has been previously shown to accurately describe the translational and rotational dynamics of anisotropic nanoparticles in suspension.<sup>4</sup> The translational and rotational diffusion coefficients can be expressed as follows

$$D_T = \frac{k_B T}{\zeta}, \zeta = \frac{3\pi\eta_0 L}{\ln(p) + \sum_{i=0}^5 a_i p^{-i}} \quad (3)$$

$$D_R = \frac{k_B T}{\xi}, \xi = \frac{\pi\eta_0 L^3}{3 \left( \ln(p) + 2 \ln(2) - \frac{11}{6} + \frac{\ln(2)}{\ln(1+p)} \left( \frac{1}{3} - 2 \ln(2) + \frac{11}{6} - \sum_{j=1}^6 b_j \right) + \sum_{j=1}^6 b_j p^{-\frac{j}{4}} \right)} \quad (4)$$

where  $\eta_0$  is the solvent viscosity,  $L$  is the length of the nanoparticle,  $p$  is the aspect ratio of the nanoparticle ( $p = L/d$ ) where  $d$  is the width,  $a_i$  are as follows:  $a_0 = 0.3863$ ,  $a_1 = 0.6863$ ,  $a_2 = -0.06250$ ,  $a_3 = -0.01042$ ,  $a_4 = -0.000651$ ,  $a_5 = 0.0005859$ ,  $b_j$  are as follows:  $b_1 = 13.04468$ ,  $b_2 = -62.6084$ ,  $b_3 = 174.0921$ ,  $b_4 = -218.8365$ ,  $b_5 = 140.26992$ ,  $b_6 = -33.27076$ .

Solving the above two equations for  $L$  and  $p$ , given the measured values of  $D_T$  and  $D_R$ , requires linearizing Equation 3 in  $L$  and substituting this into equation 4. An analogy of this approach was first proposed by Scheraga and



Mandelkern before being directly applied to DDLS in a graphical approach by Garcia de la Torre *et al.*<sup>5</sup> Instead of following a graphical approach, we numerically solved the simultaneous equations in Mathematica to find the value for  $p$  that can then be used to find  $L$  from Equation 3 or 4.<sup>6</sup> This gave dimensions of  $83 \times 48$  nm for the PVA coated GNRs.

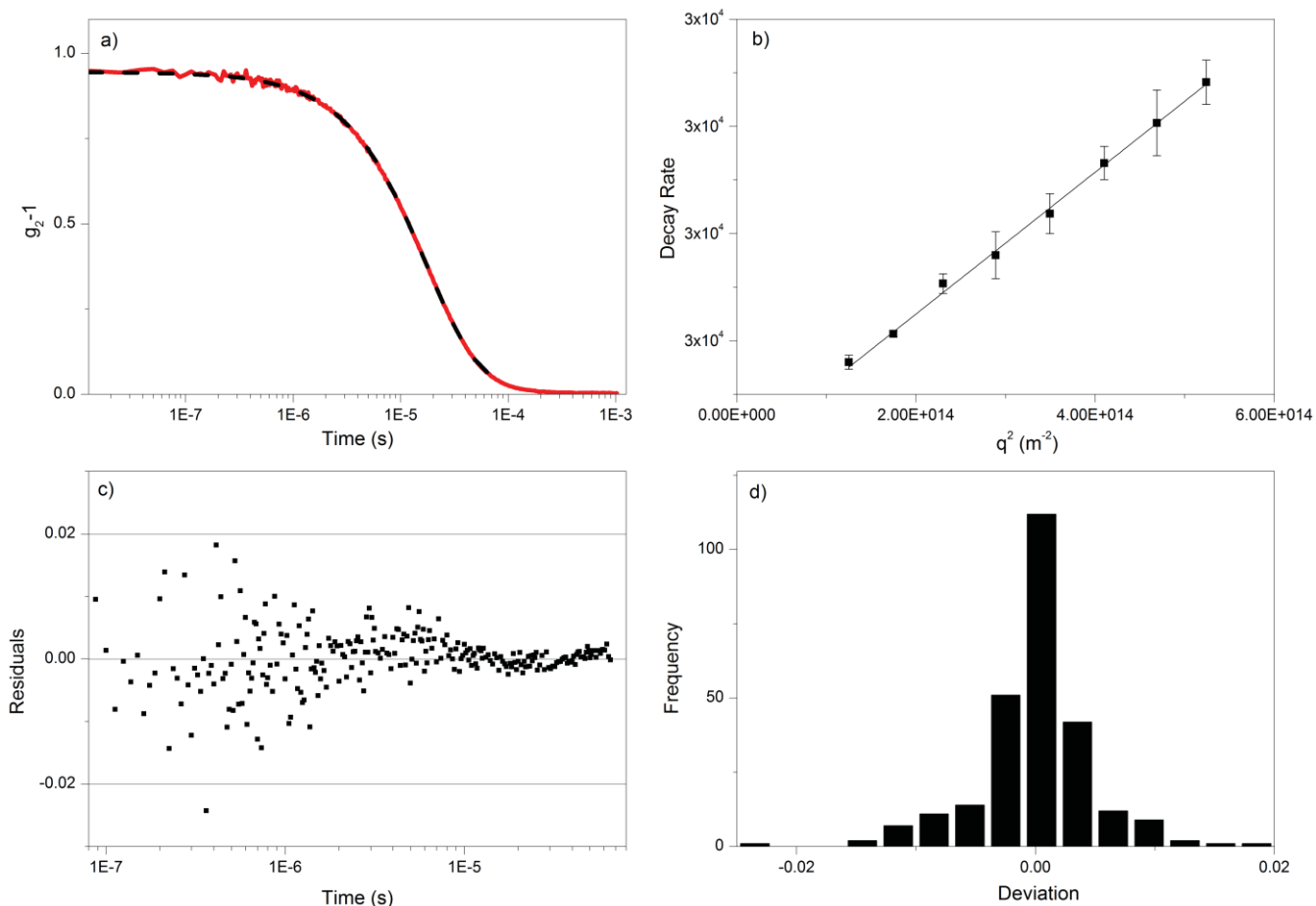


**Figure S9.** (a) Temporal autocorrelation function of GNR-PVA in water with third order cumulant best fit measured at  $90^\circ$  (dashed line). (b) Decay constant vs  $q^2$  from DDLS data of PVA coated GNRs in water at a concentration of  $67 \mu\text{g.mL}^{-1}$  at  $21^\circ\text{C}$ , with linear regression (solid line). (c) Residuals of cumulants best fit to autocorrelation function measured at  $90^\circ$ . (d) Histogram of residuals from (c).

### Control experiments

It was observed that, upon adding a concentrated suspension of CTAB-GNRs in water to a solution of PVAc in ethanol i.e. omitting the step with DMF, at the same concentrations as described above for the regular functionalization, instantaneous aggregation occurred and the precipitates sediment to the bottom of the vial. This highlights the importance of first performing a partial functionalization in DMF before transferring the GNRs to an alcoholic solution.

An additional control experiment was undertaken whereby the functionalization step in alcohol was omitted (hereafter referred to as “one-step”), and compared with the route with an extra quantity of PVAc was used in alcohol (hereafter referred to as “two-step”). From UV-Visible spectroscopy, it was evident that the two-step route conferred a higher colloidal stability likely due to higher grafting densities of PVAc on the surface of the GNRs, highlighting the importance of the functionalizing step in alcohol (Figure S9).

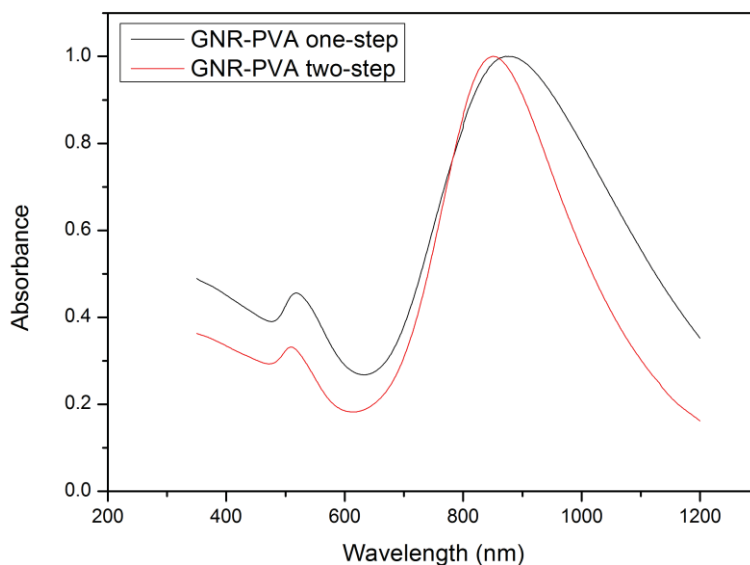


**Figure S10.** UV-Visible spectroscopy of GNRs functionalized via a one-step route in DMF, or via a two-step route in DMF and EtOH/MeOH.

### Cell Culture Experiments

Monocultures of human-monocyte derived macrophages (MDM) were isolated from human whole blood as previously described.<sup>7</sup>

The biocompatibility of PVA- and PEG-functionalized GNRs was tested through suspension exposures to primary human-monocyte derived macrophages at three different mass concentrations of gold: 10, 20, and 40  $\mu\text{g}\cdot\text{mL}^{-1}$ .

The ability of the nanorods to cause cytotoxicity after 24 h exposure was determined via the Trypan blue exclusion assay. Briefly, exposed MDM were cultured and a cell count was performed using a 1:20 dilution of Trypan Blue in cell culture media (Rosewell Park Memorial Institute medium supplemented with 10% fetal calf serum, 1% Penicillin/Streptomycin and 1% L-Glutamine). A total of 250 cells were counted, using a haemocytometer, for each exposure and percentage viability was determined from the positive control (frozen cell cultures at  $-80\text{ }^{\circ}\text{C}$  for 30 min) ( $n=3$ ).

Additionally, the ability of the nanorods to cause release of the pro-inflammatory cytokine TNF- $\alpha$  after 24 h exposure was determined with an enzyme-linked immunosorbent assay (ELISA) diagnostic kit (R&D Systems, Switzerland). As a positive control, lipopolysaccharide (LPS) at a concentration of 0.1  $\text{mg}\cdot\text{mL}^{-1}$  was used ( $n=3$ ).

In order to visualize the MDMs and qualitatively assess their morphology, laser scanning confocal microscopy (LSM) was employed. Samples were washed three times with PBS and treated with 250  $\mu\text{L}$  of Alexa Fluor<sup>®</sup> phalloidin Rhodamine (1:50 dilution) and 4',6-diamidino-2-phenylindole (DAPI stain, 1:100 dilution) for 60 min at RT in the dark. These fluorescent labels were chosen in order to stain both the cell cytoskeleton and the cell nuclei concomitantly. After completion of the staining period, samples were washed a further three times with PBS. Coverslips were then inverted and mounted onto microscope slides using Glycergel<sup>®</sup> (Dako, Carpinteria, USA) and incubated at  $4\text{ }^{\circ}\text{C}$ , in the dark, for 24 h prior to being imaged by confocal LSM (Carl Zeiss 710, Germany). All images were captured using a 63 $\times$  magnification (numerical aperture = 1.3). Following acquisition, all images were subsequently processed using the 3D multi-channel image software IMARIS (Bitplane AG, Switzerland).

### Nile Red entrapment and quantification

The entrapment of the hydrophobic dye, Nile red, was accomplished by following a similar route to that described above for the PVA-functionalization of GNRs. The functionalization was scaled up by a factor of 6, and Nile red (6.56 mg, equivalent to 50,000 dyes per GNR) was added to the to the basic methanol/ethanol mixture before hydrolysis for 2 h. The precipitated GNRs were washed with methanol until the liquid was lightly colored. Water was then added (20 mL) to redisperse the GNRs. The suspension was centrifuged twice, with redispersion in water each time.

To assess the amount of trapped dye, 4 mL of the GNRs were mixed with 3 mL of chloroform and 5  $\mu$ L of mercaptoethanol, which is known to form a self-assembled monolayer at the surface of gold nanoparticles thereby cleaving off the attached polymeric ligands. This was repeated without mercaptoethanol as a control.

The amount of dye released to the organic phase was quantified by fluorescence spectroscopy on a PTI C720 fluorometer using right angle excitation, relative to a standard curve of Nile red in chloroform. Excitation was at 465 nm and emission spectra were collected from 480 nm to 700 nm.

## References

- (1) Kinnear, C.; Dietsch, H.; Clift, M. J. D.; Endes, C.; Rothen-Rutishauser, B.; Petri-Fink, A. *Angew. Chem. Int. Ed.* **2013**, *52*, 1934–1938; *Angew. Chem.* **2013**, *125*, 1988–1992.
- (2) Ho, H. T.; Levere, M. E.; Pascual, S.; Montembault, V.; Soutif, J.-C.; Fontaine, L. *J. Polym. Sci. A Polym. Chem.* **2012**, *50*, 1657–1661.
- (3) Pecora, R. *Dynamic Light Scattering: Applications of Photon Correlation Spectroscopy*, Springer US, Boston, **1985**.
- (4) a) Norisuye, T.; Motowoka, M.; Fujita, H. *Macromolecules* **1979**, *12*, 320–323. b) Yoshizaki, T.; Yamakawa, H. *J. Chem. Phys.* **1980**, *72*, 57. c) Martchenko, I.; Dietsch, H.; Moitzi, C.; Schurtenberger, P. *J. Phys. Chem. B.* **2011**, *115*, 14838–14845.
- (5) a) Scheraga, H. A.; Mandelkern, L. *J. Am. Chem. Soc.* **1953**, *75*, 179–184. b) La Torre, J. G. de; Martinez, M. C. L.; Tirado, M. M. *Biopolymers* **1984**, *23*, 611–615.
- (6) Wolfram Research, I. *Mathematica*, Wolfram Research, Inc. Champaign, Illinois, **2010**.
- (7) Steiner, S.; Mueller, L.; Popovicheva, O. B.; Raemy, D. O.; Czerwinski, J.; Comte, P.; Mayer, A.; Gehr, P.; Rothen-Rutishauser, B.; Clift, M. J.D. *Toxicol. Lett.* **2012**, *214*, 218-225.